

An Integrated Brain ECVT and EEG System for Epilepsy Imaging

Edison Rizki Edmi^{1*}, Ihsan Muhammad Fathul^{2,3}, Rohmadi Rohmadi^{1,2}, Pratama Sra Harke⁴
and Taruno Warsito Purwo²

1. Neuroscience Center – University of Muhammadiyah Prof Dr. HAMKA, Jl. Gandaria IV No 24 Kebayoran Baru, Jakarta, INDONESIA

2. CTECH Labs Edwar Technology, Jl. Jalur Sutera Kav Spektra Blok 23 BC No 10-12, Alam Sutera, Banten, INDONESIA

3. Chiba University, 1-33 Yayoicho, Inage Ward, Chiba, 263-8522, JAPAN

4. Bandung Institute of Technology, Bandung, Jl. Ganesa No 10 Lb Siliwangi, Jawa Barat, INDONESIA

*rizkiedmiedison@uhamka.ac.id

Abstract

Localization of epileptogenic area is a fundamental step in pre-surgical evaluation. Unfortunately, phase II EEG approach has high risk due to invasiveness like infection and bleeding. Therefore, alternative approach with attention to non-invasiveness, real-time measurement and mobility is urgently needed. Brain ECVT is believed to be one of the promising neuro-imaging techniques to record human's brain activities.

In this study, we investigated the feasibility of integrated EEG and brain ECVT system. A two-electrode Brain ECVT sensor was designed to facilitate a simultaneous measurement with EEG by using COMSOL software, phantom experiment and measurement with real human in resting-state condition. Visual and power spectral density (PSD) analysis showed that ECVT excitation at 100 Hz frequency or higher does not interfere with EEG measurement. Arithmetic task was performed in human subject experiment which shows that the signal PSD during the task is higher than during relax condition in both Brain ECVT and EEG measurements. ECVT excitation at 100 Hz or higher does not interfere with EEG measurement. Brain ECVT and EEG simultaneous measurement can give similar results based on the signal power spectral density analysis.

Keywords: Brain ECVT, EEG, Epilepsy, PSD.

Introduction

Epilepsy disease has an increasing trend. Some epilepsy cases tend to be resistant to medication so that brain surgery for removing the seizure source is needed¹⁰. Localization of epileptogenic area is a fundamental step in pre-surgery evaluation⁶. If MRI fails to detect lesion or dysplasia, invasive electrode experiment has to be done which has the risks of infection and bleeding to the brain¹¹. Those risks can be lowered if the diagnostic power of non-invasive methods can be increased¹.

Scalp EEG is completely non-invasive method which is essential in epilepsy clinical diagnosis. Although considered a gold standard in pre-surgery evaluation, EEG has limitation which make it inefficient in seizure source

detection. First, seizure signal is often detected in both brain lobes. Second, the long distance from EEG electrodes to the seizure source makes interpretation more complex. Those limitations cause the lateralization success falls⁹. Functional near-infrared spectroscopy is also known as alternative neuro-imaging technology that could be used for non-invasive method to detect epileptogenic zone^{2,4}. Unfortunately, it also has limitation such as limited area to measure. Therefore, a novel technology for epilepsy imaging is needed.

Brain ECVT is known as a novel technology that could scan an object inside the human brain such as tumor⁷ and safe for human use⁸. In this study, we investigated the feasibility of an integrated EEG and brain ECVT system epilepsy imaging application.

Material and Methods

A two-electrode Brain ECVT sensor was designed to facilitate a simultaneous measurement with EEG because the existing brain ECVT helmet sensor did not allow for the insertion of EEG electrodes⁵. First, we did a simulation study using COMSOL software to determine the geometry of the ECVT electrodes which would be able to measure signal up to two centimeters below the scalp. The sensor uses planar configuration since it is the closest configuration to our two-electrode sensor setup.

After several design iterations, we chose an integrated ECVT-EEG sensor as shown in fig. 1. Each ECVT electrode has an area of two centimeters by two centimeters. The distance between the two electrodes is two centimeters. The width of the ground around the electrodes is two millimeters. The distance between the ground and the electrodes is two millimeters.

A Tektronix function generator was used to produce an excitation signal at the ECVT transmit electrode. The signal at the ECVT receive electrode was acquired by a digital storage oscilloscope Hantek. A sine wave with 1 Hz, 10 Hz, 100 Hz or 200 Hz frequency was used for the ECVT excitation. The EEG measurement was done using OpenBCI Cyton EEG acquisition system.

We performed a phantom experiment using air and water objects to test the reliability and stability of the ECVT measurement system. Since ECVT measurement is an active measurement, we had to set up an ECVT system which would

not interfere with our EEG measurement. We measured and analyzed EEG signal from a subject during relax condition without ECVT excitation and with ECVT excitation at frequencies of 1 Hz, 10 Hz, 100 Hz and 200 Hz.

For the experiment on human subjects, we used only one channel of the EEG system. The channel is located at Fp2 of the 10-20 international EEG system. The sensor placement on the subject is shown in fig. 2. The frequency used in this experiment is 100 Hz because it is the lowest ECVT excitation frequency which does not interfere with EEG measurement. The subject was aware of the purpose of the experiment. Informed consent was obtained before the start of the experiment. We chose arithmetic task for the human subject experiment since frontal lobe region is highly responsible for higher cognitive activities³.

The task required the subject to solve as many addition problems as possible in five minutes. The subject was asked to relax for 30 seconds before and after doing the arithmetic

task while the brain ECVT and EEG signals were being recorded simultaneously.

The measured signal from both brain ECVT and EEG was saved for post-processing. The post-processing of the signal was carried out using EEGLab toolbox in Matlab software. The ECVT signal was resampled to 250 Hz. Both the ECVT and EEG signals were filtered using notch filter and bandpass filter. Then, the filtered signals were analyzed based on their power spectral density (PSD).

Results and Discussion

Simulation: Three models were simulated using COMSOL software to see any difference in their electric field distributions: a) a head model without any object inside, b) a head model with an object two centimeters from the electrode surface and c) a head model with an object four centimeters from the electrode surface. The simulation visual results are shown in fig. 3. The measured capacitance from each model is detailed in table 1.

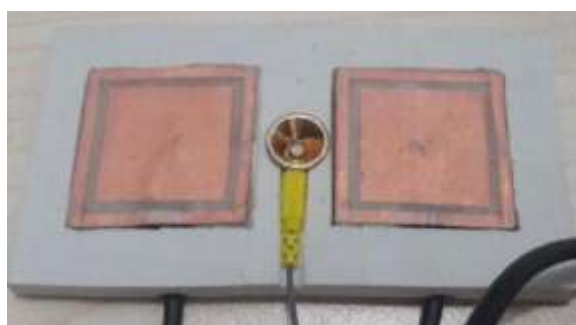


Fig. 1: An integrated Brain ECVT and EEG sensor.



Fig. 2: The sensor placement on the subject's Fp2 location: A. EEG electrode and B. integrated ECVT-EEG sensor

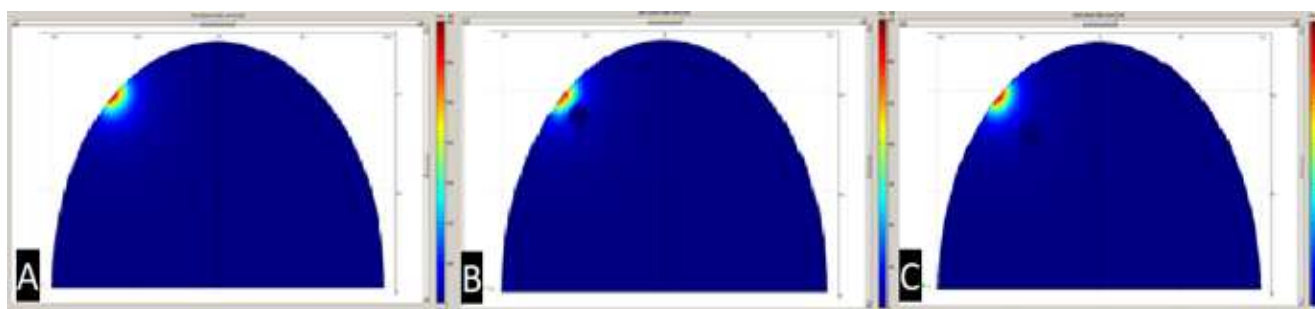


Fig. 3: Simulation visual results from: A. head model only, B. head model with object 2 cm from surface and C. head model with object 4 cm from the surface.

Table 1
Capacitance value from simulation

Parameter	Without Object	Object distance 2 cm	Object distance 4 cm
Capacitance (F)	1.658497e-13	1.767888e-13	1.680885e-13

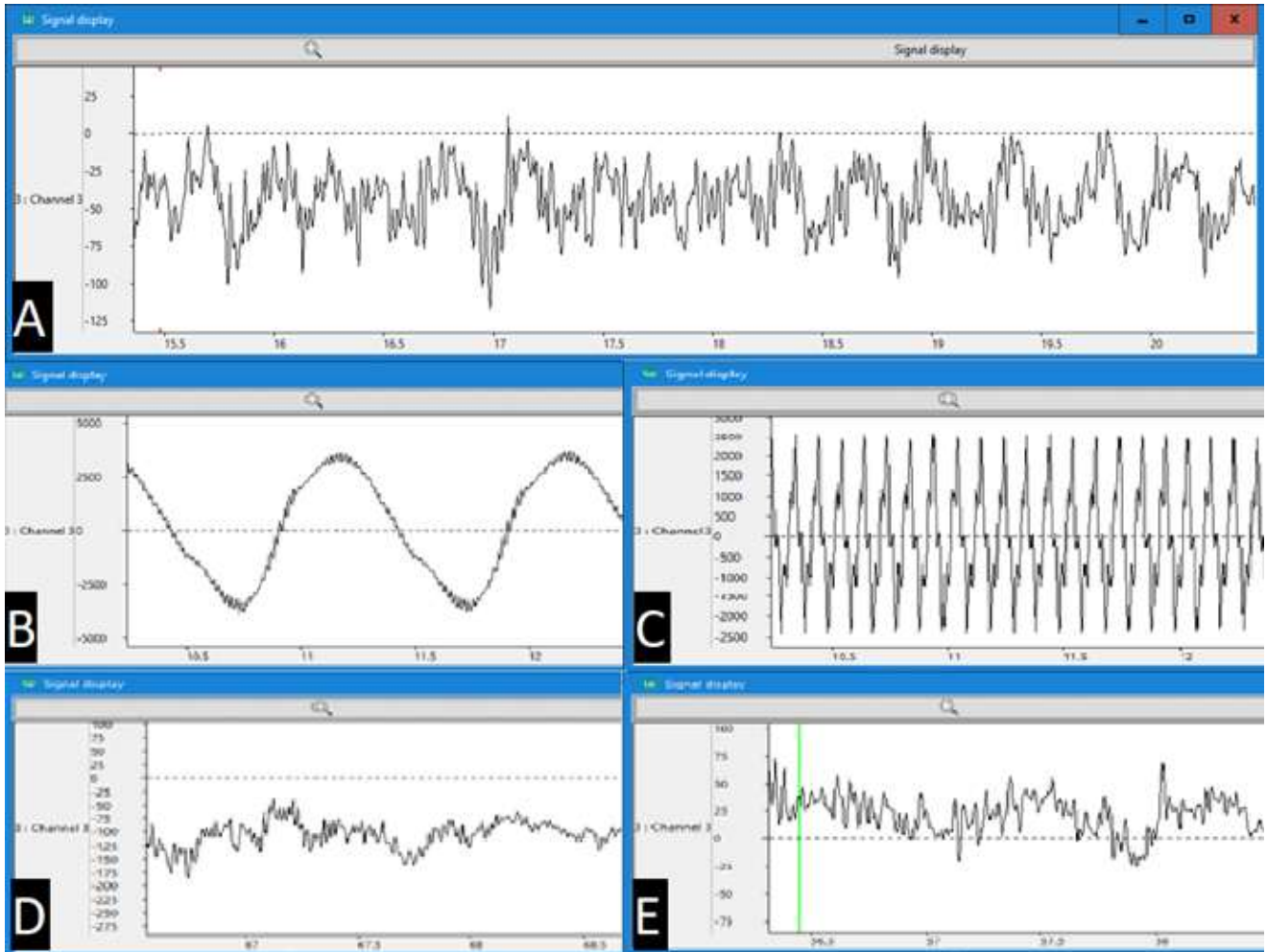


Fig. 4: EEG measured signal: A. without ECVT excitation, B. with 1 Hz excitation, C. with 10 Hz excitation, D. with 100 Hz excitation and E. with 200 Hz excitation

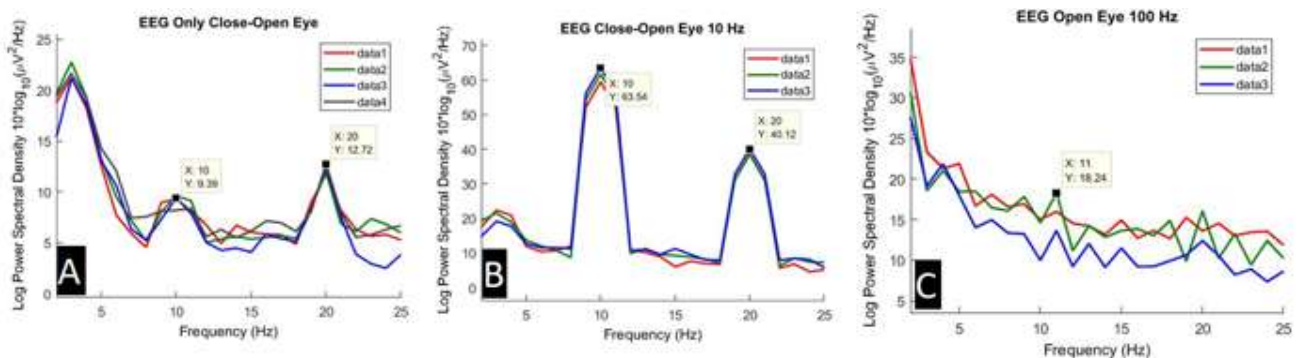


Fig. 5: PSD of EEG signal during relax condition: A. without ECVT excitation; and with B. 10 Hz and C. 100 Hz ECVT excitation.

Phantom Experiment: The phantom experiment results show that the peak of the measured signal in air object is 0.048 V while the peak of the measured signal in water object is 0.061 V.

ECVT Interference Test: The measured EEG signal without ECVT excitation is shown in fig. 4A. The measured EEG signals with ECVT excitation at 1 Hz, 10 Hz, 100 Hz and 200

Hz frequencies are shown in fig. 4B, fig. 4C, fig. 4D and fig. 4E. PSD of the EEG signals is shown in fig. 5.

Human Subject Experiment: The PSD graph of ECVT signal during arithmetic experiment is shown in fig. 6. The PSD values of the ECVT signal are detailed in table 2. The PSD graph of EEG signal during arithmetic experiment is shown in fig. 7. The PSD values of the EEG signal are detailed in table 3.

The simulation results show that for an object two centimeters from electrode surface, the electric field distribution was affected by the object. The capacitance value increased by 1.0939 pF compared to the capacitance value when there was no object near the electrode surface. When the object is four centimeters apart from the electrode surface, the electric field distribution did not change much. The

capacitance value increased only by 0.2239 pF compared to the capacitance value when there was no object near the electrode surface. Therefore, the described electrode design would be able to measure signal 2 cm apart from the electrode surface.

From the phantom experiment results, we can see that the water measurement signal is higher than air measurement which is expected since water has a higher permittivity value than air. The shape of the signal during water measurement is more similar to the excitation signal which is a sine wave with frequency 100 Hz. During air measurement, the signal shape is more distorted. The phantom experiment results show that the ECVT system can reliably distinguish between two different measurement conditions of air and water objects.

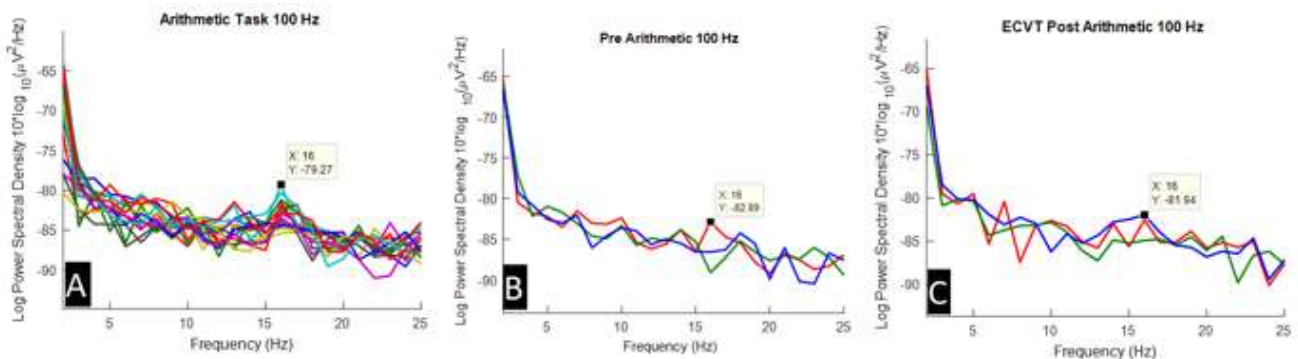


Fig. 6: PSD of ECVT signal during: A. arithmetic task, B. pre-arithmetic task and C. post-arithmetic task.

Table 2
PSD comparison of arithmetic ECVT signal

PSD ECVT pre- Arithmetic	PSD ECVT Arithmetic	PSD ECVT post-Arithmetic
-82.89	-79.27	-81.94

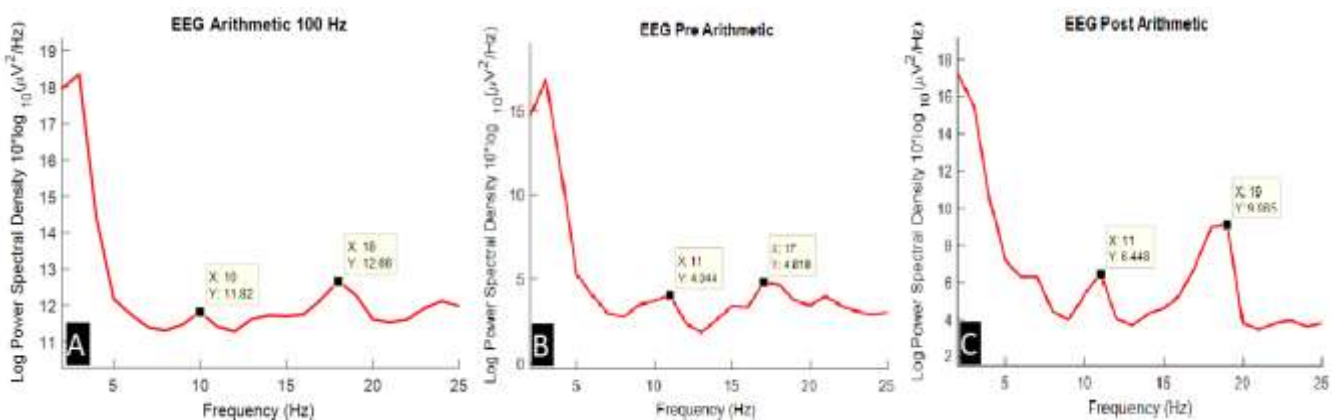


Fig. 7: PSD of EEG signal during: A. arithmetic task, B. pre-arithmetic task and C. post-arithmetic task

Table 3
PSD comparison of arithmetic EEG signal

	PSD EEG pre- Arithmetic	PSD EEG Arithmetic	PSD EEG post- Arithmetic
Frequency around 10 Hz	4.044	11.82	6.448
Frequency around 18 Hz	4.819	12.66	9.085

The EEG signal, when measured without ECVT excitation, shows the characteristics of EEG signals in general which are non-stationary, non-rhythmic and highly dynamical. The EEG signal in fig. 4A has a non-stationary characteristic. A signal which is non-stationary has trend and seasonality present within the signal which can be seen as fluctuation at a certain condition while the signal is not being rhythmic. In fig. 4A, the periodic fluctuation occurs at the amplitude change although data point values look random. Fluctuation and randomness in the data can be seen as an EEG signal.

In fig. 4B, it can be seen that EEG signal that was measured simultaneously with 1 Hz ECVT excitation has ECVT interference. The effect was visible from the presence of signal characteristics which are stationary, rhythmic and non-random which are opposite from EEG signal characteristics. It also can be seen that the frequency which arises from the EEG measurement is 1 Hz. It can be derived from the period of the signal in fig. 4B which is one second.

Fig. 4C also shows a similar case with fig. 4B where ECVT excitation at 10 Hz interfered with EEG measurement. In fig. 4C, characteristics opposite to the EEG signal characteristics can be found which are stationary, rhythmic and non-random. It also can be seen that the frequency which arises from the EEG measurement is 10 Hz. It can be evaluated from the number of peaks which is ten and the number of valleys which is ten as well within one second of measurement.

Fig. 5A shows the power spectral density of EEG signal without ECVT excitation. From the result we can see that EEG signal during opening and closing eyes has dominant PSD values at delta frequency, 10 Hz and 20 Hz. A high delta activity in the frontal area is known to have correlation with default mode network (DMN) which is a network in the brain related to resting state. Since high delta function during relax condition is considered normal, we assumed that frequency under 3 Hz will be always high during measurement. Therefore, no analysis was done for frequency less than 3 Hz.

Relax condition in general induces alpha wave in the brain. However, during the measurement, besides 10 Hz frequency which is an alpha wave, we can see 20 Hz frequency which is a beta wave. It is thought that the thinking activities were also found during measurement. The result in fig. 5A which is an EEG measurement without ECVT excitation is considered as a control and reference for the result with ECVT excitation.

The result of ECVT excitation with frequency 10 Hz during EEG measurement is shown in fig. 5B. It can be seen that the PSD at 10 Hz frequency is very high compared to fig. 5A. It means that there is a great effect to the EEG frequency distribution during ECVT excitation with frequency 10 Hz.

Since the ECVT voltage is far higher than measured EEG signal which is in the order of microvolts, the PSD value from EEG around frequency 10 Hz is thought to have been covered

by the PSD value from ECVT excitation. This result shows that ECVT excitation with frequency 0-25 Hz which is the general EEG frequency band decreases EEG measurement accuracy.

Fig. 4D shows EEG signal from a simultaneous measurement with ECVT excitation at frequency 100 Hz. From the result, we can see the EEG signal characteristic which is non-stationary (having trend and seasonality) is fulfilled by the signal data. Moreover, the measured EEG signal looks random and non-rhythmic.

Fig. 4E shows measured EEG signal with 200 Hz ECVT excitation. From the result, it can be seen that EEG signal characteristics which are non-stationary, having trend and seasonality are being fulfilled by the signal data. Besides, the measured EEG signal also has random and non-rhythmic amplitudes.

PSD analysis result from EEG measurement with 100 Hz ECVT excitation during relax condition is shown in fig. 5C. From that result, we can see that frequency peak occurs at 10 Hz frequency. That frequency shows alpha wave activity which is related to relax or rest condition. Alpha wave generally has frequency range of 7-13 Hz. The result shows that EEG measurement result with 100 Hz ECVT excitation still matches with rest condition result without ECVT excitation. The visual and PSD analysis show that there was no interference effect given by ECVT excitation at 100 Hz frequency or higher to the measured EEG signal.

From fig. 6A, fig. 6B and fig. 6C, it can be seen that PSD value of ECVT signal at 16 Hz frequency is higher during the arithmetic task compared to the PSD values during relax condition before and after arithmetic task. Frequency 16 Hz is considered a representation of beta wave activity which is related to focus and thinking activities. Based on table 2, the PSD value during arithmetic task increased 3.62 point compared to the PSD value before the task. The PSD value during relax condition after the task decreased by 2.67 point.

A similar phenomenon is found in the PSD of EEG signal shown in fig. 7A, fig. 7B and fig. 7C. The PSD values around 10 Hz and 18 Hz frequencies are higher during arithmetic task compared to the PSD values during relax condition before and after the task. During the arithmetic task, the PSD value of EEG signal around 10 Hz and 18 frequency increased by 7.776 and 7.841. During relax condition after the task, the PSD values around 10 Hz and 18 Hz frequency decreased by 5.372 and 3.575. Therefore, we can conclude that the brain ECVT and EEG give similar results during their simultaneous measurement of arithmetic task.

Conclusion

This study shows that ECVT excitation at 100 Hz or higher does not interfere with EEG measurement. Brain ECVT and EEG simultaneous measurement can give similar results based on the signal power spectral density analysis.

References

1. Alarcon G., Kissani N., Dad M., Elwes R.D., Ekanayake J., Hennessy M.J., Koutroumanidis M., Binnie C.D. and Polkey C.E., Lateralizing and Localizing Values of Ictal Onset Recorded on the Scalp: Evidence from Simultaneous Recordings with Intracranial Foramen Ovale Electrodes, *Epilepsia*, **42(11)**, 1426-37 (2001)
2. Edison R.E., Uga M., Dan I., Dan H., Tsuzuki D., Yokota H., Oguro K. and Watanabe E., Determination of Epileptic Focus Side in Mesial Temporal Lobe Epilepsy using Long-Term Noninvasive fNIRS/EEG Monitoring for Presurgical Evaluation, *Neurophotonic*, **2(2)**, 1-13 (2015)
3. Fuster J.M., Frontal Lobe and Cognitive Development, *J. Neurocytol*, **31**, 373-85 (2002)
4. Gallagher A., Lassonde M., Bastien D., Vannasing P., Lesage F., Grova C., Bouthillier A., Carmant L., Lepore F., Beland R. and Nguyen D.K., Non-Invasive Pre-Surgical Investigation of A 10 Years Old Epileptic Boy using Simultaneous EEG-NIRS, *Seizure*, **17(6)**, 576-82 (2008)
5. Ihsan M.F., Edison R.E., Pratama S.H., Saputra A., Rohmadi R. and Taruno W.P., Real-Time Measurement of Integrated Multichannel EEG-ECVT in Pre-Frontal Lobe, *EJMCM*, **7(10)**, 1343-50 (2020)
6. Ryvlin P. and Rheims S., Epilepsy Surgery: Eligibility Criteria and Presurgical Evaluation, *Dialogues Clin Neurosci*, **10(1)**, 91-103 (2008)
7. Maharani R., Edison R.E., Ihsan M.F. and Taruno W.P., Average Subtraction Method for Image Reconstruction of Brain using ECVT for Tumor Detection, *Int J Technol*, **11(5)**, 995-1004 (2020)
8. Taruno W.P., Baidillah M.R., Sulaiman R.I., Ihsan M.F., Fatmi S.E., Muhtadi A.M., Haryanto F. and Aljohani M., 4D Brain Activity Scanner using Electrical Capacitance Volume Tomography (ECVT), IEEE 10th International Symposium on Biomedical Imaging (2013)
9. Tufenkjian K. and Luders H.O., Seizure Semiology: Its Value and Limitations in Localizing the Epileptogenic Zone, *J Clin Neurol*, **8(4)**, 243-50 (2012)
10. West S., Nevitt S.J., Cotton J., Gandhi S., Weston J., Sudan A., Ramirez R. and Newton R., Surgery for Epilepsy, *Cochrane Database Syst Rev*, **6(6)**, 1-202 (2019)
11. Wong C.H., Birket J., Byth K., Dexter M., Somerville E., Gill D., Chaseling R., Fearnside M. and Bleasel A., Risk Factors for Complications during Intracranial Electrode Recording in Presurgical Evaluation of Drug Resistant Partial Epilepsy, *Acta Neurochir*, **151(1)**, 35-50 (2019).

(Received 04th February 2021, accepted 07th April 2021)